INVESTIGATION OF ANISOTROPY USING AVAZ AND ROCK MODELING IN THE WOODFORD SHALE, ANADARKO BASIN, OKLAHOMA

Alexander P. Lamb

Department of Geological Sciences
The University of Texas at Austin

ABSTRACT

This work is a seismic observation and investigation of the present in the Woodford Shale formation in the Anadarko Basin, Oklahoma. One of the main causes of anisotropy here is believed to be natural fractures. Understanding the natural fracture orientation and density is important to the development of hydraulic fracturing programs in shales producing natural gas. Dipole sonic measurements observe the Woodford to possess vertical transverse isotropy (VTI) due possibly to horizontal layering. However, an amplitude varying with azimuth (AVAZ) method that investigates horizontal transverse isotropy (HTI) was applied to 3-D seismic data and shows the dipole sonic logs may not be characterizing the HTI anisotropy observed in surface seismic data in the Woodford completely. Once this apparent contradiction was discovered, additional work to characterize the fractures was necessary. A petrophysical model of the Woodford Shale was created using multiple techniques to simulate the rock behavior. With a completed rock physics model, synthetic seismic data were generated from this model to compare to the field data. Because this synthetic seismic data has a quantified fracture density at its source, the relationship between explicit fracture parameters and AVAZ results can be established. Currently, AVAZ methods show fracture orientation and *relative* differences in fracture density and this work wants to establish quantified fracture density. Further work must be completed to finish this methodology and is detailed at the end.

INTRODUCTION

Unconventional shale reservoirs have surged in production over the last decade in North America, due mostly to the expansion and refinement of horizontal drilling and hydraulic fracturing of these formations. An important feature of these low porosity, low permeability, heterogeneous shale and tight rock formations is the existence of natural cracks and fractures, as fractures impact hydraulic fracturing programs and subsequent production. Characterizing the orientation and density of a reservoir's natural fractures requires both measurements from conventional and dipole sonic well bore logs and from seismic data. Dipole sonic measurements interact with the formation at a high frequency (2-10kHz) and this is useful for measuring P- and S-wave velocities and subsequently calculating details such as water saturation, clay content, and density. However, this high frequency has a limited sampling range from the borehole due to

attenuation and may not characterize volumetric properties such as fracture density and dominant fracture orientation with the accuracy necessary. The seismic data and its longer wavelengths may help to resolve these larger scale properties. Specifically, this work investigates the Woodford Shale formation in the Anadarko Basin in western Oklahoma for horizontal transverse isotropy and natural fractures. The Woodford shale is one of several Devonian black shales in North America under exploration or development of shale gas (Harris 2011). Over 300 horizontal Woodford Shale wells have been completed just in the Anadarko Basin since 2008 (Caldwell, 2011). Knowing both fracture density (the number of fractures per unit volume) and fracture orientation, expressed as the dominant azimuthal direction, may contribute to productive exploitation of the Woodford. Ideally, a horizontal drilling and hydraulic fracturing program would cross normal to higher-density areas of fractures to improve permeability and therefore production. Higher permeability, and high values of the seismic attribute brittleness, maximizes effectiveness of these drilling and fracking programs (Wylie 2007).

Initial analysis of the dipole sonic measurements of velocity indicates the presence of vertical transverse isotropy (VTI) and no significant horizontal transverse isotropy (HTI). This VTI result may not be surprising given the natural layering of most shales. Analysis of seismic data using amplitude varying with azimuth (AVAZ) methods, however, indicates that the Woodford does indeed possess HTI, further proving the usefulness of seismic data to complete the depiction of unconventional reservoirs. AVAZ methods have been used by numerous authors to investigate fracture parameters (Gray et al, 1999, 2000, Hall and Kendall, 2000, Li, 1999, Lynn et al, 1996, MacBeth and Lynn, 2001, Pérez et al, 1999). Results from AVAZ give the azimuthal orientation and the relative fracture intensity. To further characterize the natural fractures of the Woodford beyond AVAZ, I employ a combination of several petrophysical models to model this formation.

Modeling of this formation was initially performed by estimating the composition and lithology of the Woodford from borehole measurements. Starting with this background as an isotropic block, the method of Hashin-Strickman-Walpole bounds (Berryman, 1995) was performed to estimate values of rock stiffnesses at formation porosity, verified by other borehole measurements. Now working with an isotropic model including porosity, cracks were introduced to the model using the Hudson crack model (1980), while again being constrained by dipole sonic measurements. Finally, fluid saturation was included in the model through the method of Brown and Korringa (1975). Through the combination of these petrophysical methods, I now had a model of the anisotropic Woodford Shale characterized by explicit composition, fracture parameters, and fluid saturation. Synthetic seismograms generated using ANIVEC (Mallick and Frazier 1988), allows for AVAZ methods to be performed and compared to the field seismic data. This will allow AVAZ results to give a fracture orientation and, indirectly, a numeric fracture density.

WELL DATA

Figure 1 shows well-log data from a well in Canadian County in the Anadarko Basin, OK. Curves included are (from left to right) the gamma ray (*GR*), water saturation (S_w), bulk density (ρ), P-wave velocity (V_p), S-wave velocity (V_s), P-wave S-wave ratio (Vp/Vs), bulk modulus (K) and shear modulus (μ). The S_w, K, and μ curves are calculated indirectly. The

Woodford Shale exists between 12973 and 13245 ft., and it is distinguishable in the *GR*, ρ, V_p, V_s, K, and μ logs. Above the Woodford formation sits the Mississippian Limestone and below sits the Hunton Limestone. In the Woodford, the average bulk density of ρ is ~2.45 g/cm^3, while the average V_p is ~3.3 km/s and V_s is ~2 km/s. This low density has been observed by previous studies of organic black shales (Vernik and Nur, 1992; Vernik and Liu, 1997).

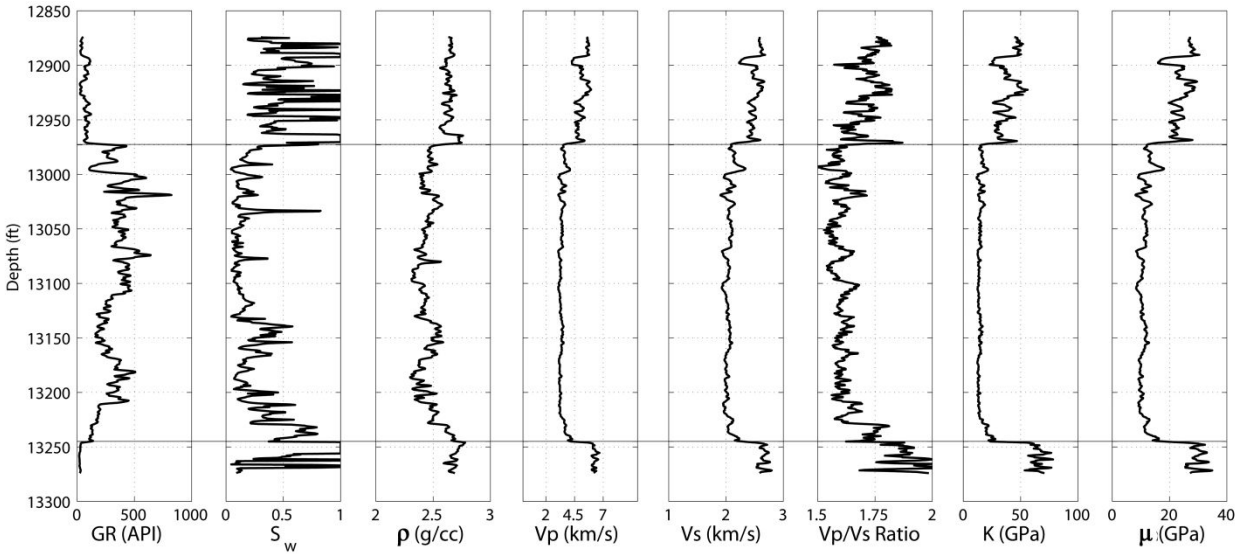

Figure 1. Well data that samples the Woodford Shale. The Woodford lies between 12973 and 13245 ft. depth. Well logs and calculated traces are (left to right) gamma ray, water saturation, bulk density, P-wave velocity, S-wave velocity, velocity (Vp/Vs) ratio, bulk modulus, and shear modulus.

ANISOTROPY BACKGROUND

The term anisotropy is used to describe a material's response being directionally dependent. In other words: along different axes there are differences in the material's measured parameters (the opposite of isotropy, which is measurement similarity in all directions). The existence of anisotropy, usually due to fractures in either the horizontal and/or vertical directions, has measureable effects on a material's stiffness and seismic velocity. If not corrected for, anisotropy has been shown to affect interpretation results (Cheadle et al. 1991). Therefore, if one of these parameters can be measured in different directions, we can infer something about the fractures that exist in the media. The location and density of these fractures has a large implication for the success of a drilling and fracking completion operations and reservoir exploitation, as these fractures may be conduits for fluid flow. Two idealized types of anisotropy are discussed here: vertical transverse isotropy (VTI) where the axis of symmetry is vertical due perhaps to horizontal bedding and horizontal transverse isotropy (HTI) where the axis of symmetry is horizontal due perhaps to vertical fracturing (Figure 2). Anisotropy is known to prefer a certain azimuthal orientation due to regional horizontal stresses in basins forcing closed cracks not in a certain azimuth (Mueller 1992).

Investigation of shear waves show that birefringence (splitting) of the shear wave due to anisotropy could be related to fracture intensity and orientation (Tatham and McCormack 1991). Shear waves traveling through an anisotropic medium will polarize into two directions: parallel

to the predominant fracture direction (S1) and orthogonal to this direction (S2). S1 is seen to have a higher velocity than S2. Currently, S1 and S2 are measured in dipole sonic borehole logs as well as seismic data, the results of which will be shown later.

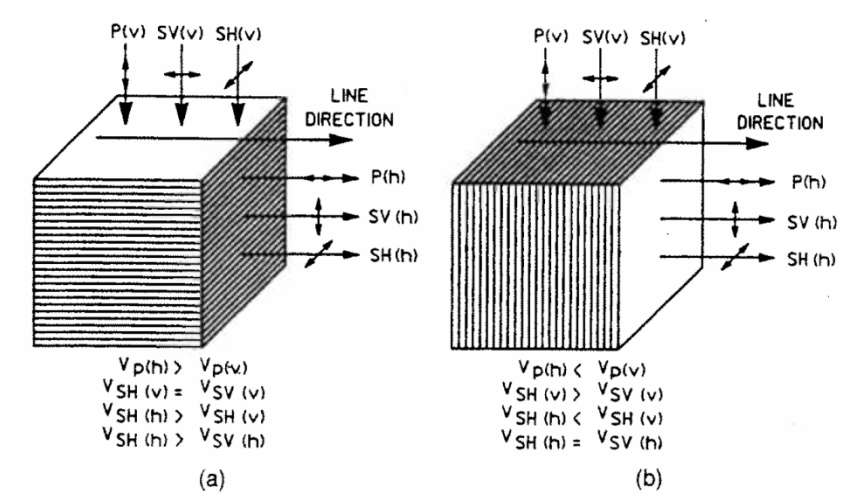

Figure 2. Examples of transverse isotropy. a) Vertical transverse isotropy (VTI) has a faster horizontal P-wave velocity b) Horizontal transverse isotropy (HTI) shows S1 (SH(v)) as faster than S2 (SV(v)). [From Tatham and McCormack 1991]

AMPLITUDE VARYING WITH AZIMUTH (AVAZ) BACKGROUND

P-wave reflection amplitudes are sensitive to anisotropy induced by vertical fractures (HTI) and can be affected both as a function of offset and azimuth. This investigation of amplitude varying with azimuth (AVAZ) allows us to infer orientation and relative fracture density. Investigating reflection amplitudes has advantages over investigating traveltime differences because AVAZ concentrates on contrasts at a single reflector, while traveltime methods are affected by overlying layers (Hall and Kendall, 2000). Another advantage of AVAZ is the ability to detect fracture parameters using only P-wave data.

Fundamentally, AVAZ is a 3-D extension of varying reflection amplitudes with offset (AVO), which was described in detail by Castagna and Backus (1993). Zoepprittz (1919) originally described the full equations of P-wave reflectivity between two isotropic half-spaces, and then Shuey (1985) approximated these equations for small angles of incidence (<35 degrees) with the formula:

$$Rp(\theta) = A + B\sin^2(\theta) + C\sin^2(\theta)\tan^2(\theta) \quad (1)$$

where $Rp(\theta)$ is the P-wave reflection coefficient at an incident angle θ, A is the reflection coefficient at normal incidence (known as AVO intercept), B is known as the AVO gradient, and C is a third term that dominates at larger angles as the critical angle is approached. AVO gradient is a function of AVO intercept and Poisson's ratio σ, which in turn is a function of the ratio of P-wave and S-wave velocities. These coefficients were further simplified by Thomsen (1990) as:

$$A = \Delta Z/(2\bar{Z}) \quad (2a)$$

$$B = \frac{1}{2}\left(\frac{\Delta V_p}{\overline{V_p}} - \frac{\left(\frac{2\overline{V_s}}{\overline{V_p}}\right)^2 \Delta\mu}{\mu}\right) \tag{2b}$$

$$C = 1/2\left(\frac{\Delta V_p}{\overline{V_p}}\right) \tag{2c}$$

where V_p is P-wave velocity, V_s is S-wave velocity, Z is the acoustic impedance (ρV_p) and μ is the shear modulus. Terms with a bar indicate the average value.

If the medium contains no azimuthal anisotropy, the AVO terms will be equal for all source-receiver pairs. If the medium is azimuthally anisotropic, however, the AVO response will also be a function of azimuth. Rüger (1996) modified the previous AVO equations to include azimuthal anisotropy and show reflection amplitudes as:

$$A = \Delta Z_0/(2\overline{Z_0}) \tag{3a}$$

$$B = \frac{1}{2}\left(\frac{\Delta V_{p0}}{\overline{V_{p0}}} - \frac{\left(\frac{2\overline{V_{s0}}}{\overline{V_{p0}}}\right)^2 \Delta\mu_0}{\mu_0} + \Delta\delta\right) \tag{3b}$$

$$C = 1/2\left(\frac{\Delta V_{p0}}{\overline{V_{p0}}} + \Delta\epsilon\right) \tag{3c}$$

where $\Delta\delta$ and $\Delta\varepsilon$ are contrasts in Thomsen parameters for HTI media and all previous quantities now with a '*0*' subscript indicate the vertical portion specifically.

The AVO gradient term *B* has been shown in HTI media to have an elliptical form, but only for shorter offsets (<35 degrees) (Rüger, 1996 and Jenner, 2001). This is due to the third term dominating at longer offsets and negating the requirements of ellipticity. Therefore, for these shorter offsets, the equation can be rewritten as:

$$Rp(\theta) = A + B\sin^2(\theta) \tag{4a}$$

where the AVO gradient term B is now

$$B = \frac{1}{2}\left(\frac{\Delta V_{p0}}{\overline{V_{p0}}} - \frac{\left(\frac{2\overline{V_{s0}}}{\overline{V_{p0}}}\right)^2 \Delta\mu_0}{\mu_0} + \Delta\delta(\varphi)\right) \tag{4b}$$

$$\Delta\delta(\varphi) = \delta_1 \cos^2(\varphi - \varphi_0) + \delta_2 \sin^2(\varphi - \varphi_0) \tag{4c}$$

The anisotropic term $\delta(\varphi)$ has an elliptical form with δ_1 and δ_2 as the maximum and minimum axes of the ellipse respectively, and φ is the azimuth describing the strike of the vertical fractures direction (Figure 3). Therefore, the fracture orientation can be determined by fitting an ellipse to the AVO gradient term. Also, the proportion between the maximum and minimum ellipse axes of the ellipse can be used to estimate of relative fracture intensity (Montoya 2002).

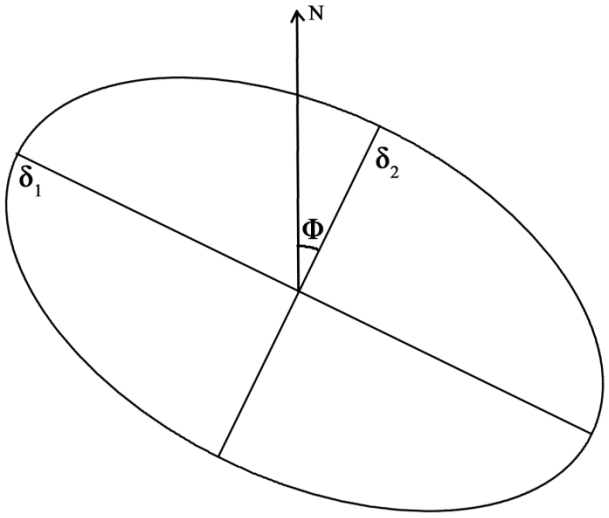

Figure 3. The anisotropic term δ(φ) has an elliptical form with δ_1 and δ_2 as the maximum and minimum axes of the ellipse respectively, and φ is the azimuth of the fracture orientation (Modified from Montoya 2002)

WELL DATA SHOWING VERTICAL TRANSVERSE ISOTROPY (VTI)

The suite of measurements contained in the dipole sonic borehole logs was extensive, and included P-wave velocity for the vertical and horizontal directions, as well as a 'fast' and 'slow' shear wave corresponding to S1 and S2 velocity in the horizontal direction. The horizontal P-wave measurement was made from analysis of the Stoneley wave inside the borehole to extract the C_{11} stiffness tensor element (preliminary investigations into the details of this proprietary measurement were unsuccessful).

In a VTI medium, the horizontal P-wave velocity exceeds the vertical P-wave velocity, and there is negligible difference between the S1 and S2 velocities, as each horizontal bedding layer would be isotropic (refer to anisotropic background). In Figure 4, log velocity data is shown. The curve titled '*Vp Diff %*' is the percentage difference between the Vp and Vp horizontal measurements. Similarly with '*S Diff %',* this is the percentage difference between S1 and S2. This figure demonstrates exactly what we expect in a VTI medium: namely the Vp difference is large and the S difference is negligible. With the Vp difference, we observe that the vertical (normal to bedding) P-wave velocity is lower, which has been observed before in organic black shales (Vernik and Nur, 1992; Vernik and Liu, 1997). In fact, due to the nature of bedding in shales, many properties are even assumed to behave as a VTI medium (Brevik, 2007). While these borehole results demonstrate these assumptions are correct, the seismic data, operating on an entirely different resolution, will show further investigation is needed.

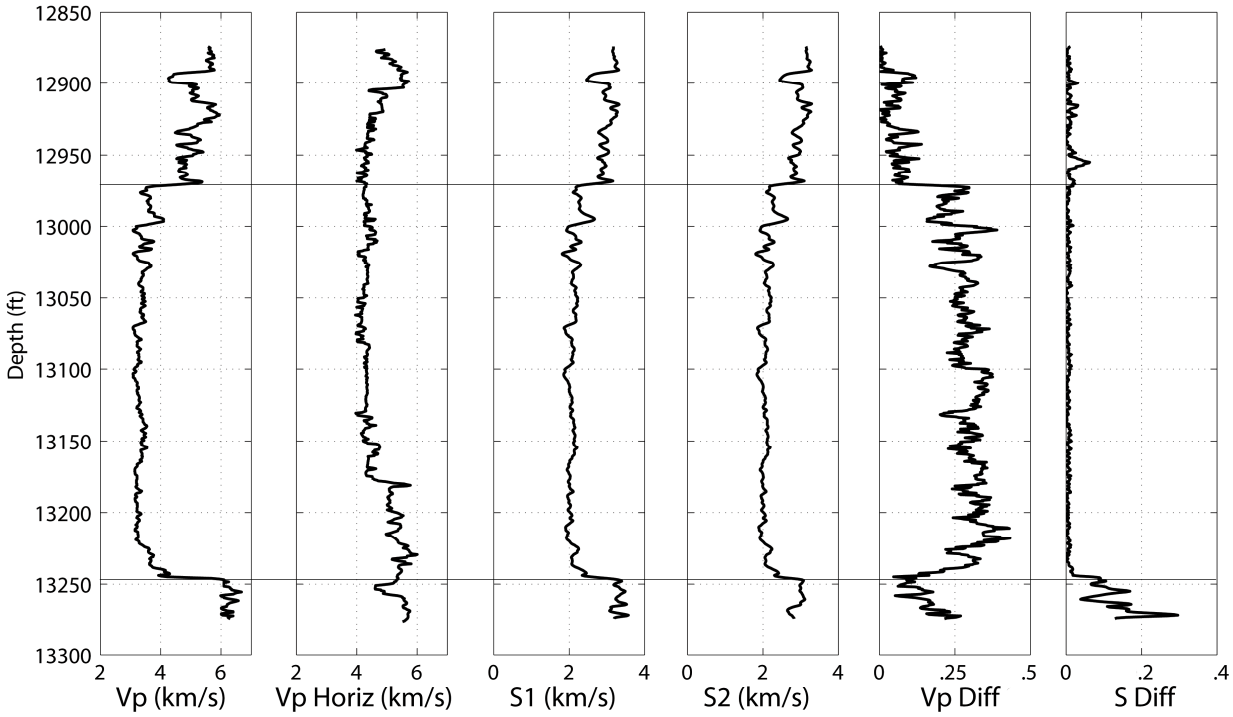

Figure 4. Curves displaying the velocity measurements in the well. From left to right: p-wave velocity, horizontal p-wave velocity, S1 velocity, S2 velocity, percentage difference between p-wave and horizontal p-wave, percentage difference between S1 and S2. These results, high Vp diff % and minimal S diff %, in the Woodford (12973-13245 ft.) indicate the presence of VTI.

SEISMIC DATA

The seismic data were acquired over a ~14 square mile patch in Canadian County, Oklahoma in the Anadarko Basin. While this work concentrates on vertical component P-wave data, 3-component data were collected as well to a depth of 14000 ft. Processed, post-stack data and raw pre-stack data was provided and both were used in this work. The pre-stack data was processed while preserving amplitudes, a necessary requirement of AVAZ analysis. This requirement did not allow full migration of the pre-stack data due to contamination of reflection amplitudes; although others are investigating methods to avoid this (Zheng 2011), it is not covered in the recent investigation.

Results from the post-stack data were used to tie the seismic to depth and pick the interpreted horizons for the Woodford Shale. A well tie was performed with the dipole sonic log measurements generating a synthetic trace. This correlation was very good (>90%) and established the depth and thickness of the Woodford Shale. From this information, the top and bottom of the Woodford Shale was picked for the entire survey.

AVAZ ANALYSIS OF SEISMIC DATA

The horizons picked from the post-stack data were transferred and verified on the pre-stack data showing the top and bottom of the Woodford Shale. To perform AVAZ analysis on

these data, it was gathered into 36 azimuthal wedges ranging in 10 degree increments from 0-360 degrees. Each wedge was paired with its complement (+180 degrees) wedge. (Figure 5)

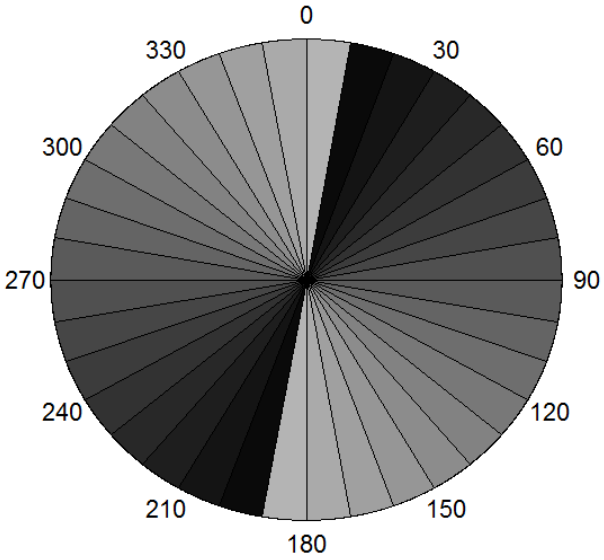

Figure 5. Visualization of azimuthal wedges used for AVAZ analysis. A wedge and its corresponding wedge complement (+180 degrees) were grouped and analyzed.

Each of these azimuthal gathers was converted from an offset gather to an angle gather based on time-depth conversion from the well dipole sonic log (Figure 6). All traces are now shown as depth vs. incident angle. The need for the traces to be a function of angle is a requirement of AVAZ.

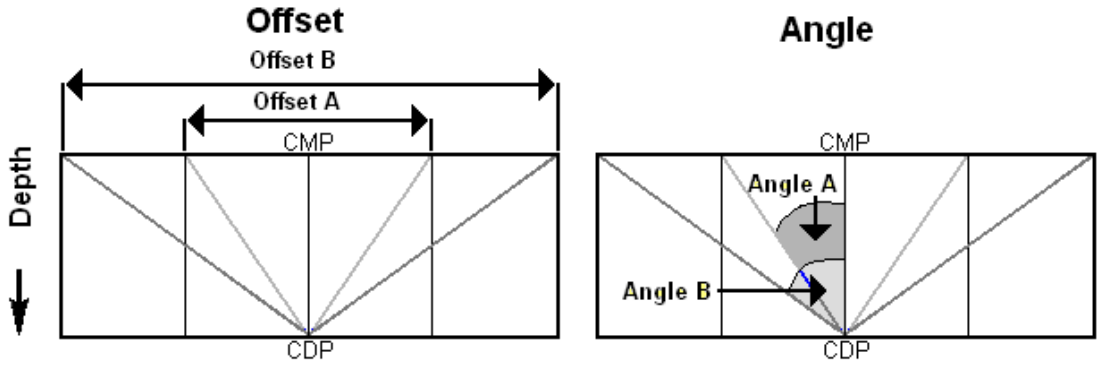

Figure 6. Visualization of angle gathers [From Hampson Russell Assistant - Angle Gathers]

Once the gathering into azimuthal groups and angle gather transformation was performed, AVO gradient analysis could be completed. For each azimuth, an AVO intercept and gradient was estimated at the depth corresponding to the top of the Woodford (~2230 ms). Due to the sectioning of azimuths into 10 degree blocks, the results graph is variable, but still shows an interpretable azimuthal dependence (Figure 7). This result is a key indicator of the existence of HTI, in direct contrast to the borehole logs. Obviously, further analysis will be performed on multiple source-receiver combinations to determine relative fracture density spatially.

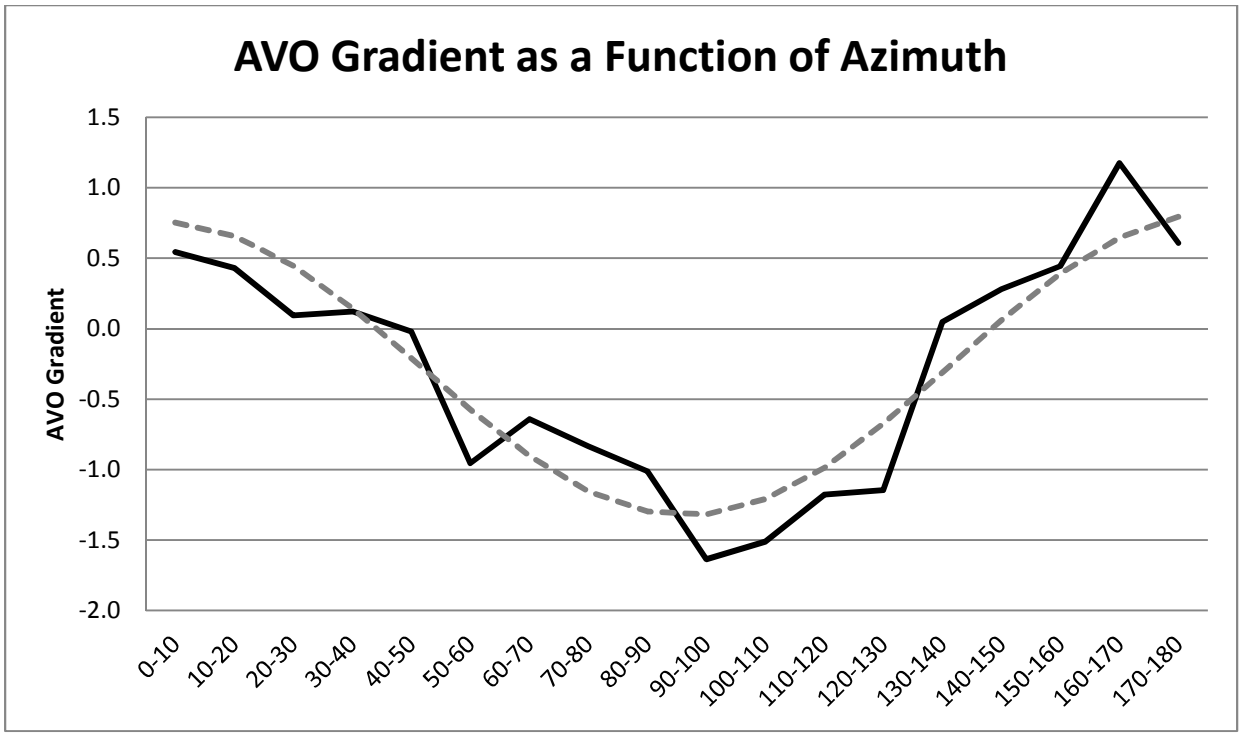

Figure 7. Graph showing AVO Gradient (B) as a function of azimuth (solid line), grouped into 10 degree blocks after AVAZ analysis, and a sinusoidal fit (dashed line),

Ellipse Fitting

An ellipse can be fit to the AVO vs. azimuth data to show orientation and relative fracture density. As with this one set of data (for this specific inline and crossline survey position), the fracture density will not mean much yet. However, the orientation is our first glimpse into the dominant fracture direction. Using MATLAB, an ellipse was fit using least squares to the AVO gradient. This ellipse is shown below in Figure 8.

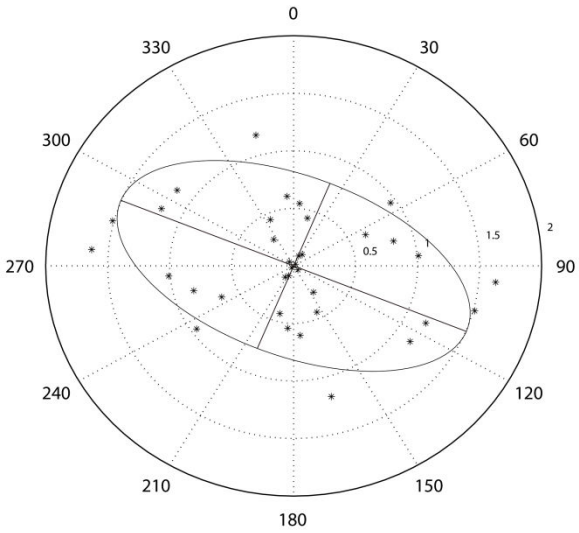

Figure 8. Ellipse fitting to the AVAZ results. Trend shows a SW/NE (minor axis) for the fracture orientation.

The ellipse shows an orientation of SW/NE, in agreement with other preliminary results from Gupta (2011). To further investigate the fracture density, and move beyond relative to quantitative fracture density estimates, this work explores a petrophysical model of the Woodford that attempts to establish a relationship between a numeric fracture density and the ellipticity of the AVO gradient ellipse.

ROCK PHYSICS MODELING

Four main elements comprise the rock physics modeling in this study. First, an estimation of the Woodford Shale composition is made based on mineralogical borehole logs. From this composition, rock stiffnesses are estimated in the context of Hashin-Strickman-Walpole bounds (Berryman, 1995). Second, the introduction to the model of penny-shaped cracks using of the Hudson cracked media model. Lastly, fluid saturation is added to the model using the methods of Brown and Korringa (1975). Altogether, this procedure develops a rock model of a porous, cracked, partially fluid-saturated rock analogous to the Woodford Shale. This becomes the basis for our investigation into fracture density and its effect on AVO gradient. Previous studies have inverted sonic and dipole sonic log data for the stiffness tensor using effective medium theory (Bayuk et al. 2008), but the model presented here attempts to build upwards.

Composition Estimate

To estimate the Woodford Shale's composition, firstly I used fractions of carbonate, quartz, clay, pyrite, and kerogen. Mineralogical logs in the borehole suite measured volume fractions of each of these minerals, and I scaled them to complete the mineralogical model. The entire Woodford mineralogy with depth is shown in Figure 9:

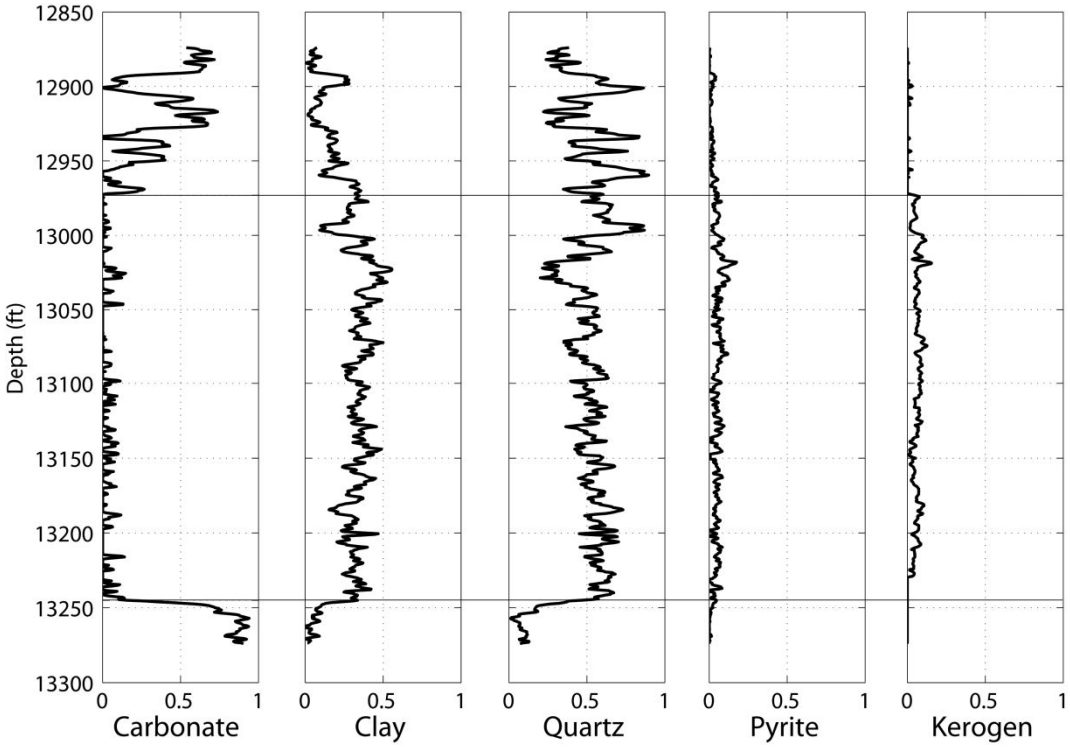

Figure 9. Composition of Calcite, Clay, Quartz, Pyrite, and Kerogen. Horizontal lines denote the Woodford

From this figure, we can observe the distinct differences between the Woodford (approximately equal parts of clay minerals and quartz) and the surrounding limestones (Mississippian above and Hunton below), specifically the presence of kerogen and increase in clay content. The higher siliceous quartz content in the Woodford has been shown to readily enhance fracturing (Guo, 2007) because of the increased rigidity. The entire Woodford mineralogy, including minor pyrite fractions, is used to develop further stages of this model.

From the approximate lithologies, combined with the water saturation log and bulk density, we can estimate the porosity of Woodford Shale (Equation 5). Volumetrically averaging mineral densities gives ρ_m and assuming the fluid density ρ_f is a mixture of water and gas governed by the water saturation log, the porosity can be calculated. Table 1 shows the data used.

$$\rho_b = (1-\phi)\rho_m + \phi\rho_f \tag{5}$$

	Bulk Modulus (GPA)	Shear Modulus (GPA)	Density (g/cm^3)
Calcite	77	32	2.75
Clay	21	7	2.60
Quartz	37	44	2.65
Pyrite	143	121	4.87
Kerogen	2.9	2.7	1.30
Gas	0.07	0	0.20
Water	2.6	0	1.05

Table 1. Material data used for composition estimates (Mavko et al., 2009)

Hashin-Strickman-Walpole

From the previous section, we have an estimation of the mineral composition with corresponding isotropic bulk modulus and shear modulus as a function of depth, similar to a borehole log. To correct these moduli for the presence of porosity, the Hashin-Strickman-Walpole bounds (Berryman, 1995) are used to estimate the bounds of K and μ as a function of porosity for each measurement. The upper (HSW+) and lower (HSW-) bounds of K and μ are calculated (Equations 6a-6e):

$$\mu^{HSW+} = \left[\frac{\phi}{\mu_f+X} + \sum_{k=1}^{M}\frac{(1-\phi)f_k}{\mu_k+X}\right]^{-1} - X \tag{6a}$$

$$X = \frac{\mu_{\max}}{6}\left(\frac{9K_{max}+8\mu_{max}}{K_{max}+2\mu_{max}}\right) \tag{6b}$$

$$\mu^{HSW-} = \frac{\mu_{min}}{6}\left(\frac{9K_{min}+8\mu_{\min}}{K_{min}+2\mu_{min}}\right) \tag{6c}$$

$$K^{HSW+} = \left[\frac{\phi}{K_f+\frac{4}{3}\mu_{max}} + \sum_{k=1}^{M}\frac{(1-\phi)f_k}{K_k+\frac{4}{3}\mu_{max}}\right]^{-1} - \frac{4}{3}\mu_{max} \quad (6d)$$

$$K^{HSW-} = \left[\frac{\phi}{K_f} + \sum_{k=1}^{M}\frac{(1-\phi)f_k}{K_k}\right]^{-1} - \frac{4}{3}\mu_{min} \quad (6e)$$

After the upper and lower bounds were calculated for each depth, the mean of these two bounds was used to have K and u as a function of porosity. Porosity is known, however, from our calculations (Equation 5). Therefore, we directly have a new value for porosity-corrected K and u, K' and u'.

Hudson Crack Model

The Hudson crack model introduces thin, penny-shaped ellipsoidal cracks into an isotropic medium. An effective moduli C_{ij}^{eff} is calculated from the isotropic background moduli C_{ij}^{0} corrected by C_{ij}^{1} (shown below in Equations 7a-e). With a given crack density and aspect ratio, Hudson limits the crack porosity (Equation 7h). The Hudson model returns a modified stiffness tensor C_{ij}^{eff}. For this model, we assume the cracks to have small aspect ratios (in this case, 0.01).

$$C_{ij}^{eff} = C_{ij}^{0} + C_{ij}^{1} \quad (7)$$

$$C_{11}^{1} = -\frac{\lambda^2}{\mu}\epsilon U_3, \quad C_{13}^{1} = -\frac{\lambda(\lambda+2\mu)}{\mu}\epsilon U_3, \quad C_{33}^{1} = -\frac{(\lambda+2\mu)^2}{\mu}\epsilon U_3, \quad C_{44}^{1} = -\mu\epsilon U_1, \quad C_{66}^{1} = 0 \text{ (7a-e)}$$

In this instance of dry cracks (saturation is modeled later), U_1 and U_3 are given as:

$$U_1 = \frac{16(\lambda+2\mu)}{3(3\lambda+4\mu)} \qquad U_3 = \frac{4(\lambda+2\mu)}{(3(\lambda+\mu))} \quad (7f\text{-}g)$$

$$\epsilon = \frac{3\phi^{crack}}{4\pi\alpha} \leq 0.1 \quad (7h)$$

Brown and Korringa Fluid Saturation

After the model incorporates the cracks from the Hudson model, the material is still considered 'dry'. To incorporate fluids, the Brown and Korringa fluid substitution method is used, which takes the original stiffness tensor, rock moduli, porosity, and the bulk modulus of the fluid. From this a correct stiffness tensor is given.

$$s_{ijkl}^{sat} = s_{ijkl}^{dry} - \frac{\left(s_{ijaa}^{dry} - s_{ijaa}^{0}\right)\left(s_{bbkl}^{dry} - s_{bbkl}^{0}\right)}{\left(s_{ccdd}^{dry} - s_{ccdd}^{0}\right) + \phi(\beta_{fl} - \beta_0)} \quad (8)$$

Where s_{ijkl}^{dry} is the effective elastic compliance tensor element of dry rock, s_{ijkl}^{sat} is the effective elastic compliance element of rock saturated with pore fluid, s_{ijkl}^{0} is the effective elastic compliance element of the solid mineral, β_{fl} is the fluid compressibility ($1/K_{fl}$), β_0 is the mineral compressibility ($s_{\alpha\alpha\gamma\gamma}^{0} = 1/K_0$), and φ is the porosity.

Rock Physics Discussion

The resulting final stiffness tensor represents the Woodford Shale corrected for porosity, cracks, and fluid saturation. It represents an HTI medium with natural fractures at a specific crack density and aspect ratio, a specific lithology and is the basis for the synthetic seismic data generated. The overlying layer, the Mississippian limestone, was modeled as an isotropic medium with stiffness tensor determined by the borehole log measurements of P-wave and S-wave velocity.

SYNTHETIC SEISMIC DATA

The ANIVEC program, developed by Mallick and Frazer (1988), computes synthetic seismograms using a layercake-based Earth model wherein the user specifies the number of layers and each layer's specific stiffness tensor. From this, ANIVEC computes a three-component seismic response. For this work, we will begin with just the P-wave data similar to our AVAZ analysis previously. As we are not concerned with the orientation using ANIVEC, only density, we do not have to match the AVO gradient ellipse in *direction*. However, the fracture density affects the ellipse shape, and this work attempts to match a fracture density with the field seismic data. Future work is required to complete this analysis, as not all azimuths of synthetic data have been currently analyzed.

FUTURE WORK

Future progress involving this rock physics model and AVAZ could break down the Woodford into multiple layers, as commonly it is divided geologically into three layers. This may prove difficult with AVAZ, however, as three reflectors are not osberved in most source-receiver pairs. Also, an investigation using the multi-component shear-wave seismic data would allow observation of the splitting of the S1 and S2 waves. With multi-component data, mode-converted PS waves could be observed and traveltime differences could lead to more complete characterizations of the fracture parameters. With more layers of AVAZ analysis, a fracture density map could evolve into a fracture density volume, allowing for more sophisticated drilling programs to take advantage of 3-D highs in fracture density. Expanding the AVAZ analysis and combining with attenuation analysis, Clark *et al.* (2009) limits the uncertainty in fracture orientation determination. Other work by Gupta (2011) investigates newly-developed geometric attributes (reflector convergence) combined with seismic attributes such as curvature and coherence to analyze fractures in the Woodford.

CONCLUSIONS

This work shows an investigation of anisotropy in the Woodford Shale that gives incongruent results using borehole logs vs. seismic data. Sonic and dipole sonic measurements, with their higher frequency, may sample too small a rock volume to give complete descriptions of the rock's overall anisotropic nature. Seismic data and its long wavelengths may not be useful

in detailing incremental rock properties, but may in fact be advantageous for volumetric properties such as fracture density and orientation. AVAZ was shown to be a method for calculating fracture orientation and relative density, but the rock physics models will be responsible for quantifying that density. Limitations given by one borehole log through the Woodford certainly constrain the solution given here, but the methodology can easily be expanded once more data become available. In the end, characterizing the fracture orientation and density would be valuable to the horizontal drilling of these unconventional reservoirs in the search of enhanced permeability.

Well log data and pre-stack seismic data comprised the bulk of this work. Therefore, unstated uncertainties can arise due to lack of core calibration and lack of clarity in seismic data wherein reflection-altering processes are disallowed. An investigation of the bottom reflector of the Woodford is not treated here, but would help give insight into the anisotropic nature of the formation as well.

ACKNOWLEDGEMENTS

The sponsors of the EDGER Forum at the University of Texas at Austin supported this work. Thanks go to Devon Energy and Cimarex for access to the borehole and seismic data.

REFERENCES

Bayuk, I., M. Ammerman, and E. Chesnokov, 2008, Upscaling of elastic properties of anisotropic sedimentary rocks: Journal Geophysics International, **172**, 842–860.

Berryman, J. G., 1995, Mixture theories for rocks. *In Rock Physics and Phase Relations: a Handbook of Physical Constants*, ed. T. J. Ahrens. Washington, DC: American Geophysical Union.

Brevik, I., 2007, Documentation and quantification of velocity anisotropy in shales using wireline log measurements. The Leading Edge. March 2007. p. 272-277

Brown, R. and Korringa, J., 1975. On the dependence of the elastic properties of a porous rock on the compressibility of the pore fluid, *Geophys.*, **40**, 608-616

Caldwell, C., 2011, Lithostratigraphy of the Woodford Shale, Anadarko Basin, West-Central Oklahoma, AAPG Search and Discovery Article #50518

Castagna, J. P., and Backus M., 1993, Offset-dependent reflectivity: theory and practice of AVO analysis: *Society of Exploration Geophysicists, Investigation in Geophysics,* No. 8, pp. 3-36

Cheadle, S. P., Brown, R. J., and Lawton, D. C., (1991) Orthorhombic anisotropy: A physical modeling study, *Geophysics*, **56**, 1603-1630

Clark, R. A., P. M. Benson, A. J. Carter, and C. A. Guerrero Moreno, 2009, Anisotropic P-wave attenuation measured from a multi-azimuth surface seismic reflection survey: Geophysical Prospecting, 57, 835–845.

Gray, F.D. and Head, K.J., 2000, Fracture Detection in the Manderson Field: A 3D AVAZ Case History: The Leading Edge, Vol. 19, No. 11, 1214-1221.

Guo, Y., K. Zhang, and K. J. Marfurt, 2010. Seismic attribute illumination of Woodford Shale faults and fractures, Arkoma Basin, OK. 80th annual SEG meeting, Expanded Abstracts, 1372-1376.

Gupta, N., 2011, Seismic characterization of the Woodford Shale in the Anadarko Basin, 81st annual SEG meeting, Expanded Abstracts.

Hall, S.A., and Kendall J.M., 2000, Constraining the interpretation of AVOA for fracture characterization, Anisotropy 2000: Fractures, Converted Waves and Case Studies, Proceedings of 9IWSA: *SEG Open Publication*, no. 6, pp. 107-144

Harris, N. 2011, Mechanical Anisotropy in the Woodford Shale, Permian Basin: Origin, magnitude and scale. The Leading Edge. March 2011 p284-291.

Hudson, J. A., 1980, Overall properties of a cracked solid: Mathematical proceedings of the Cambridge Philosophical Society, **88**, 371–384.

Jenner, E., 2001, Azimuthal anisotropy of 3-D compressional wave seismic data, Weyburn field, Saskatchewan, Canada, Ph.D. Thesis: *Colorado School of Mines*, 197p

Li, X. -Y., 1999, Fracture detection using azimuthal variation of P-wave moveout from orthogonal seismic survey lines: Geophysics, Soc. of Expl. Geophys., 64, 1193-1201.

Lynn, H.B., Simon, K.M. and Bates, C.R., 1996, Correlation between P-wave AVOA and S-wave traveltime anisotropy in a naturally fractured gas reservoir: The Leading Edge, 15, 8, 931-935.

MacBeth, C. and Lynn, H., 2001, Mapping fractures and stress using full-offset full-azimuth 3D PP data: 71st Ann. Internat. Mtg: Soc. of Expl. Geophys., 110-113.

Mavko, G., Mukerji, T., Dvorkin, J., 2009, The rock physics handbook: tools for seismic analysis of porous media, Cambridge University Press

Montoya, P., 2002, Characterization of a Fractured Sandstone Reservoir From Core to 3D Seismic Analysis in the Tacata Field, Eastern Maturin Basin, Venezuela. M.S. Thesis: *University of Texas*

Mueller, Michael C., 1992, Using shear waves to predict lateral variability in vertical fracture intensity: The Leading Edge, **11**, no. 02, 29-35

Pérez, M., 1996, Detection of fracture orientation using azimuthal variation of P-wave AVO responses. *Geophys*. **64**, 1253-1265

Rüger, A., 1996, Reflection coefficient and azimuthal AVO analysis in anisotropic media, Ph.D. Thesis: *Colorado School of Mines*

Shuey, R.T., 1985, A simplification of the Zoeppritz equations: *Geophysics*, v. 50, pp. 609-614

Tatham, R.H., and M.D. McCormack, 1991, Multicomponent seismology in petroleum exploration, Investigation in Geophysics Series Vol. 6, Society of Exploration Geophysicists.

Thomsen, L., 1990, Poisson was not a geophysicist: *The Leading Edge*, v. 9, no. 12, pp 27-29

Vernik, L. and A. Nur, 1992, Ultrasonic velocity and anisotropy of hydrocarbon source rocks: Geophysics, **57**, no. 5, 727‑735

Vernik, L. and X. Liu, 1997, Velocity anisotropy in shales: A petrophysical study: Geophysics, **62**, no. 2, 521‑532

Wylie, G., 2007, Advances in fracs and fluids improve tight-gas production. Oil & Gas Journal. December 2007.

Zheng, Y. 2011, Fracture Analysis with Interpolation Before Prestack Migration. 2011 CSPG CSEG CWLS Convention.

Zoeppritz, K., 1919, Erdhebenwellen VIIIB, On the reflection and propagation of seismic waves *Göttinger Nachr*., I, 66-84

Mallick, S., and Frazer, L.N., 1988, Rapid computation of multioffset vertical seismic profile synthetic seismograms for layered media, Geophysics, 53, 479-491